arXiv:1608.02501v1 [quant-ph] 8 Aug 2016

WKB propagators in position and momentum space for a linear potential with a "ceiling" boundary

T A Zapata[1,3] **and S A Fulling**[1,2]

[1] Department of Physics, Texas A&M University, College Station, Texas, USA
[2] Department of Mathematics, Texas A&M University, College Station, Texas, 77843-3368, USA
[3] Present address: Department of Electrical and Computer Engineering, Texas A&M University, College Station, Texas, 77843-3128, USA

E-mail: todd-austin-zapata@tamu.edu, fulling@math.tamu.edu

Abstract. As a model for the semiclassical analysis of quantum-mechanical systems with both potentials and boundary conditions, we construct the WKB propagator for a linear potential sloping away from an impenetrable boundary. First, we find all classical paths from point y to point x in time t and calculate the corresponding action and amplitude functions. A large part of space-time turns out to be classically inaccessible, and the boundary of this region is a caustic of an unusual type, where the amplitude vanishes instead of diverging. We show that this curve is the limit of caustics in the usual sense when the reflecting boundary is approximated by steeply rising smooth potentials. Then, to improve the WKB approximation we construct the propagator for initial data in momentum space; this requires classifying the interesting variety of classical paths with initial momentum p arriving at x after time t. The two approximate propagators are compared by applying them to Gaussian initial packets by numerical integration; the results show physically expected behavior, with advantages to the momentum-based propagator in the classically forbidden regime (large t).

1. Introduction

The propagator of a quantum-mechanical system is the integral kernel (Green function) that solves the initial-value problem for its time-dependent Schrödinger equation:

$$\mathrm{i}\hbar\,\frac{\partial\psi}{\partial t} = H\psi \Longleftrightarrow \psi(\mathbf{x},t) = \int U(\mathbf{x},\mathbf{y},t)\psi(\mathbf{y},0)\,\mathrm{d}\mathbf{y}. \tag{1}$$

The semiclassical or WKB ansatz, in its simplest form, is to write

$$U(\mathbf{x},\mathbf{y},t) = A(\mathbf{d_y})\mathrm{e}^{\mathrm{i}S(\mathbf{d_y})/\hbar} \qquad (\mathbf{d_y} \equiv [(\mathbf{y},0),(\mathbf{x},t)]) \tag{2}$$

and to choose $S((\mathbf{y},s),(\mathbf{x},t))$ and $A((\mathbf{y},s),(\mathbf{x},t))$ so that (1) is satisfied up to order $\hbar^2$. The *action* S and *amplitude* A can be constructed by solving the classical equations of motion and integrating certain first-order differential equations along the resulting paths (trajectories) in space-time.

The classical-mechanical problem that must be solved in this construction is a two-point boundary-value problem, since the initial point $\mathbf{y}$, the final point $\mathbf{x}$, and the elapsed time $t-s$ (for time-independent Hamiltonians) are prescribed. This problem is generally not well-posed, in the sense that for certain data there may be more than one path, for others no path at all ("classically forbidden regions"), and at still other points A may become infinite. This last phenomenon is called a *caustic*, which technically can be defined as a set where the mapping to $\mathbf{x}$ from the initial momentum $\mathbf{p}$ (at $\mathbf{y}$) fails to be a diffeomorphism. Ordinarily a caustic represents a breakdown of the WKB approximation (although the WKB propagator of a harmonic oscillator is exact, despite having caustics). A semiclassical solution that is accurate in the vicinity of a caustic often can be found by transforming, at least temporarily, into a momentum representation [1, 2, 3].

The literature of semiclassical approximation is well developed for Hamiltonians $H = \mathbf{p}^2/2m + V(\mathbf{x})$ (and much more general phase-space functions) in $\mathbf{R}^n$ without boundaries, as considered in the classic paper of Van Vleck [4] and many other works, such as [1, 2, 3]. The case $H = -\nabla^2$, with a reflecting boundary but no potential, is also well studied (for example in [5], or indeed in all geometrical optics). But there has been little or no attention to problems with both boundaries and potentials, although the small-t asymptotic expansion of U, or rather its close relative the heat kernel, is well known for very general operators with boundaries, potentials, Riemannian curvature and external gauge fields [6, 7].

In this paper we construct in detail two WKB propagators for a simple system: The configuration space is one-dimensional, the positive x axis; the potential is a decreasing, linear function of x; the boundary condition at the origin is perfect reflection (Dirichlet). Because classically this potential describes a force pulling a particle away from the boundary, we think of the force as gravitational and call this boundary a *ceiling*. (Of course, it could at least equally well be a constant electrostatic force. The problem also arises in the study of diffraction by a smooth convex obstacle [8].) The extension to dimension 3 with a flat ceiling is immediate, since the propagator factors and the

WKB approximation for the transverse propagator is exact. This model already presents many of the features of the general case: Since space-time is two-dimensional, the full multidimensional WKB theory (using tools from Hamilton–Jacobi theory) is needed. The WKB approximation is not exact for the wave reflected from the ceiling, so this model is not "trivial" in the sense that the WKB propagator for a linear or quadratic potential in all of $\mathbf{R}^n$ is. The spectrum is continuous, which complicates the solution of the Schrödinger equation by separation of variables; on the other hand, no classical path strikes the ceiling more than once, so the WKB solution is relatively simple. (The spectrum is also unbounded below, but only because of what happens as $x \to +\infty$, so no physical pathology results.) In the semiclassical construction of $U(x, y, t)$ a certain region of space-time is classically forbidden, because if t is too large compared to x and y, "a ball cannot be thrown from y to x in exact time t because the ceiling gets in the way". The boundary of that region is not a caustic in the usual sense, because the amplitudes do not diverge there; however, the amplitude of the wave reflected from the ceiling does go to 0 there, indicating a nondiffeomorphic dynamics, and its derivatives do become singular there. To investigate semiclassically what happens on and beyond this critical curve, we construct the propagator $U(x, p, t)$ that yields, in analogy to (1), the wave function $\psi(x, t)$ in terms of the initial wave function in momentum space, $\hat{\psi}(p, 0)$. (This step is the paper's most original contribution to the literature.) The momentum-based calculation seems to be superior to the position-based one, at least for certain initial data and times, because it does not falsely predict that the propagator is identically 0 at large t.

In the remainder of this introduction we set up notation and review some basic formalism. In section 2 we find all solutions of the classical two-point boundary value problem for initial position y (and given destination (x, t)). If t is sufficiently small, there are always two solutions, one that never reaches the ceiling and one that bounces off it. If t is too large, there are no solutions. There is a unique solution on the *critical curve*, (12). We calculate the action and amplitude for both the direct and the bounce path, thereby obtaining an approximate propagator $U(x, y, t)$ adequate for points inside (and not too near) the critical curve. In section 3 we elucidate the critical curve by replacing the ceiling by a smooth but rapidly rising potential. Numerical solutions for families of classical paths reveal caustics (in the familiar sense) that converge, in the limit of an infinitely steep potential, to the union of the critical curve and the portion of the ceiling that gets struck by the bounce paths. In section 4 we solve the two-point boundary value problem for initial momentum p in place of y; in this case the structure of the set of allowed paths is more complicated. Again there is a mild caustic-like behavior (compare (108) with (70)), but it has moved to a different part of phase space. Again the actions and amplitudes are calculated. The resulting approximate propagator $U(x, p, t)$, when applied to an initial wave packet concentrated at values of y for which (x, t) would be in the classically forbidden region or on the critical curve, gives a plausible, nonvanishing value to the wave function. We have not proved error bounds, but in section 5 we offer some preliminary numerical calculations on Gaussian initial packets that show the

expected physical behaviors.

Although an exact analytical solution for the propagator $U(x, y, t)$ exists as an integral of Airy functions (see section 1.3), it is difficult (for the present authors, at least) to use in numerical work, so we have no trustworthy comparisons to present. In contrast, the related problem with a *floor* instead of a ceiling has been often studied (e.g., [9, 10, 11]); it has a discrete spectrum. In that case it is the WKB approach that runs into complications, because there are infinitely many classical paths to sum over.

The detailed solution of the ceiling problem with linear potential, presented in this paper, points the way to a prescription for handling boundaries in problems with arbitrary potentials (and perhaps ultimately also higher-dimensional problems with curved boundaries). This "localization" strategy is analogous to the treatment of diffraction from corners by applying the formulas for diffraction by an infinite straight wedge [12], and it provided the original motivation for this work.

This paper, especially section 4 and section 5, is based on the Master of Science thesis of the first author [13]. A preliminary account of the conclusions in section 2 and section 3 was presented by the second author at QMath8, Taxco, Mexico, December 2001.

1.1. The classical system

The system considered in this article is a 1-dimensional one with an impenetrable barrier at the origin and a linear potential,

$$V(q) = -\alpha q. \tag{3}$$

Here q represents the position of the particle, and α characterizes the strength and direction of the potential. For α greater than zero the barrier is a "ceiling" and the particle may bounce off at most once. If α is less than zero then the barrier will act as a floor, and will have, in principle, an infinite number of bounces. This article considers the ceiling case for two different types of data,

- Initial position, y, and final position, x;
- Initial momentum, p, and final position, x.

The final time is t, and when it is necessary to consider an initial time other than 0, it is denoted s. The time parameter for a path interpolating between these data is τ, and the corresponding position variable is q; occasionally the notation $p(\tau)$ is needed for the momentum at some point along the path.

The equation governing the dynamics of the classical system and its general solution are

$$\frac{\mathrm{d}^2 q}{\mathrm{d}\tau^2} = \frac{\alpha}{m}\,, \qquad q(\tau) = \frac{\alpha}{2m}\,\tau^2 + A\tau + B. \tag{4}$$

The constants of integration, A and B, are determined from the initial data considered. For bounce trajectories two subsidiary solutions are required, $q_1(\tau)$ and $q_2(\tau)$, corresponding to the dynamics before and after the collision, respectively. An

extra condition must be placed on the bounce trajectories so that the momenta of these paths at the ceiling are equal in magnitude and opposite in direction. If b is the time at which the particle ricochets, this condition is

$$p_1(b) = -p_2(b). \tag{5}$$

Unless otherwise stated the remainder of the paper will use the natural units

$$\hbar \equiv 1, \qquad m \equiv \tfrac{1}{2}, \qquad \alpha \equiv 1. \tag{6}$$

Note that when the last two of these equations are in force, position will have the same dimensionality as time squared, and momentum will have the same dimensionality as time:

$$[x] = [t]^2, \qquad [p] = [t], \tag{7}$$

in contrast to the more familiar situation where $\hbar$ and c (but not m) are dimensionless and hence $[x] = [t]$, $[p] = [t]^{-1}$. Also, the velocity is twice the momentum; although this is classically weird, it makes the quantum formulas more elegant.

1.2. The classical solutions

The preliminary quest is to determine all possible trajectories connecting the initial data (p, s) or (y, s) with the final data (x, t), and the corresponding constraints. For notational simplicity the two-point data will be abbreviated

$$\mathbf{x}_y \equiv [(y, s), (x, t)], \qquad \mathbf{x}_p \equiv [(p, s), (x, t)].$$

There are three types of non-bounce trajectories to consider:

(i) trajectories that initially and finally move away from the ceiling: $p \equiv p_s \in (0, \infty)$ and $p_{\rm f} \in (0, \infty)$;

(ii) trajectories that initially and finally move toward the ceiling: $p \equiv p_s \in (-\infty, 0)$ and $p_{\rm f} \in (-\infty, 0)$;

(iii) trajectories that initially move toward the ceiling, and end moving away from the ceiling: $p_0 \in (-\infty, 0)$ and $p_{\rm f} \in (0, \infty)$.

A plot of these three types of trajectory is in figure 1. The time at which the particle's momentum is zero, n, governs the transition between motion toward the ceiling and away from the ceiling for type (iii) trajectories.

There are certain boundary trajectories, which are helpful in analyzing the more general situations. Trajectories of type (i) are separated from trajectories of types (ii) and (iii) by a trajectory whose initial momentum is zero. It has initial position

$$\tilde{y} \equiv x - t^2, \tag{8}$$

so that $q(\tau) = \tau^2 + x - t^2$. In this case, if $x > t^2$ the initial position will be on the physical side of the ceiling, but for $x < t^2$ the initial position will not be physical. Also, keeping the final data fixed implies that if an initial positive momentum is given to this trajectory, then the initial position must be moved closer to the ceiling. Conversely, for

Figure 1. Three types of non-bounce trajectories with equal initial data, y, and final time, t. The only variable is the final position, x. $xd1$ represents the final position of a type (i) trajectory; $xd2$ the final position for type (ii); and xt that for a turning trajectory, type (iii).

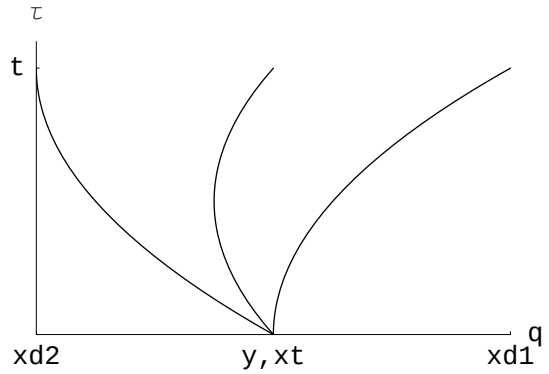

an initial negative momentum for a trajectory of type (ii), the initial position will be pushed away from the ceiling. Therefore, one has $y < \tilde{y}$ for type (i) and $y > \tilde{y}$ for types (ii) and (iii).

The linear potential implies that the momentum gained by the particle is equal to the time of flight, τ (recall (7)), and the total momentum of the trajectory at any time is

$$\tau + p. \tag{9}$$

Therefore, in case (iii) the time at which the particle will turn around is

$$n = -p. \tag{10}$$

The distance from the initial point to the turning point for a trajectory where $t = n$ is

$$\Delta = -\int_0^n v(\tau)\,\mathrm{d}\tau = -2\int_0^{-p} (p+\tau)\,\mathrm{d}\tau = p^2 = t^2. \tag{11}$$

The negative sign occurs because the velocity is inherently negative during the initial segment of the motion considered. The boundary between cases (ii) and (iii) is marked by $y = \Delta$, or $t = \sqrt{y}$.

For some initial and final data, both a direct (non-bounce) trajectory and a more energetic bounce trajectory exist; see figure 2. The critical trajectories for the bounce paths are the type (iii) trajectories with zero momentum at the ceiling, corresponding to zero energy. All other trajectories for the bounce case have energy greater than zero, since those with negative energy can never reach the ceiling. Also, all allowed trajectories of type (iii) have negative energy, since otherwise they would pass through the ceiling. A way to view the construction of bounce trajectories is to join two trajectories at the ceiling which there obey equation (5); one trajectory has the correct initial data, and the other the final data. Therefore, the critical trajectory occurs when these two trajectories are the same; the bounce trajectory becomes an ordinary path of type (iii). A particle in a linear potential beginning at the ceiling with zero energy (and therefore

Figure 2. General bounce trajectory (dotted line) connecting initial data, y, to the final data, x, in the same time, t, as a direct trajectory (solid line).

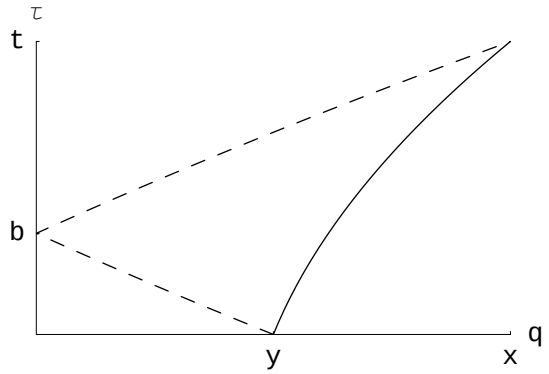

Figure 3. Generic family of bounce trajectories with the same initial position and final time. The final position, x, is varying. The critical trajectory is dashed, and bc denotes the time of bounce for this trajectory, xc denotes the final position. The region above and to the left of the dashed curve is classically inaccessible.

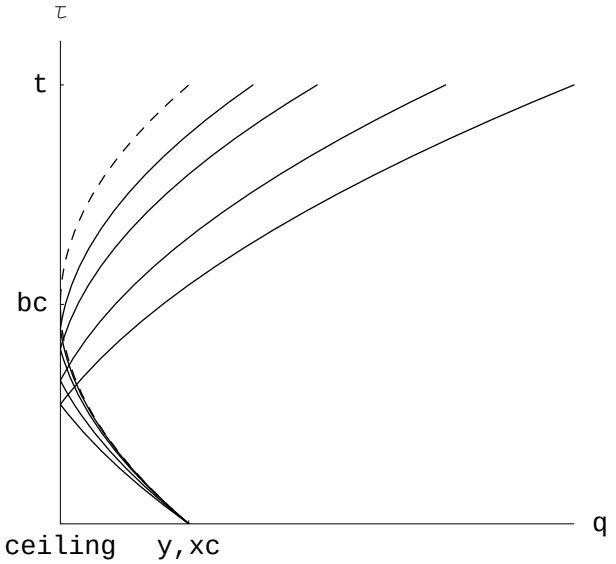

zero initial momentum) will end at location x with momentum $\sqrt{x}$. Conversely, if the particle arrives at the ceiling with zero energy, its momentum at the starting point, y, must have been $-\sqrt{y}$. Therefore, by (9) the total momentum the particle will gain on the critical bounce trajectory is

$$\sqrt{x} + \sqrt{y} = t. \tag{12}$$

This equation characterizes the critical trajectory. As will be seen in detail in section 2, the critical trajectory marks the boundary between the region of space-time points (x, t) that can be connected to y by classical paths and those that cannot (see figure 3).

1.3. The quantum theory

The time-dependent Schrödinger equation satisfied by our particle, in the units (6), is

$$-\frac{\partial^2\psi}{\partial x^2} - x\psi = \mathrm{i}\,\frac{\partial\psi}{\partial t}\,. \tag{13}$$

The ceiling is implemented by restricting x to positive values and imposing the boundary condition $\psi(0,t)=0$.

The solutions of the time-independent Schrödinger equation,

$$-\frac{\mathrm{d}^2\psi_E}{\mathrm{d}x^2} - x\psi_E = E\psi_E\,, \tag{14}$$

are Airy functions, $\mathrm{Ai}(-x-E)$ and $\mathrm{Bi}(-x-E)$ and their linear combinations. The spectrum is continuous and unbounded above and below: $-\infty < E < \infty$.

It is known (e.g., [14]) that the propagator that solves the initial-value problem for (13) is

$$U(x,y,t) = \int_{-\infty}^{\infty} \psi_E(x)\psi_E(y)e^{-iEt}\rho(E)\,\mathrm{d}E \tag{15}$$

with

$$\psi_E(x) = \pi[\mathrm{Bi}(-E)\,\mathrm{Ai}(-x-E) - \mathrm{Ai}(-E)\,\mathrm{Bi}(-x-E)], \tag{16}$$

$$\rho(E) = \pi^{-2}[\mathrm{Ai}(-E)^2 + \mathrm{Bi}(-E)^2]^{-1}. \tag{17}$$

The integral (15) is very oscillatory and hence hard to use in practice.

On the other hand, for a free particle (that is, when (13) holds on the whole real line, with no boundary), the corresponding formula,

$$U_\infty(x,y,t) = \int_{-\infty}^{\infty} \mathrm{Ai}(-x-E)\,\mathrm{Ai}(-y-E)e^{-iEt}\,\mathrm{d}E, \tag{18}$$

is known in closed form (e.g., [15], [16, and references therein]):

$$U_{\mathrm{free}}(t,x,y) = (4\pi\mathrm{i}t)^{-1/2}\,e^{\mathrm{i}(x-y)^2/4t + \mathrm{i}(x+y)t/2 - \mathrm{i}t^3/12}. \tag{19}$$

We rederive this formula in passing in (72a).

For completeness, note that in the presence of a floor instead of a ceiling (that is, $\alpha=-1$), the spectrum is discrete and the propagator is easily seen to take the form

$$U_{\mathrm{floor}}(x,y,t) = \sum_{n=1}^{\infty} \mathrm{Ai}'(-E_n)^{-2}\,\mathrm{Ai}(x-E_n)\,\mathrm{Ai}(y-E_n)e^{-iE_nt}, \tag{20}$$

where the E_n are the roots of $\mathrm{Ai}(-E_n)=0$. The WKB solution in this case would be difficult, because of the need to sum over many reflected classical paths (as the particle bounces inside the potential well).

1.4. The WKB ansatz

In this section we reintroduce the constants $\hbar$ and m and allow for a higher-dimensional configuration space; thus x becomes $\mathbf{x}$, and we usually omit the arguments y, s, and t. The mathematical correspondence between classical physics and the quantum propagator begins with the ansatz

$$U(\mathbf{x}) = \mathrm{e}^{\frac{\mathrm{i}}{\hbar}S(\mathbf{x})} \sum_{j=0}^{\infty} \left(\frac{\mathrm{i}}{\hbar}\right)^{-j} A_j(\mathbf{x}) \tag{21}$$

for a solution to the time-dependent Schrödinger equation

$$-\frac{\hbar^2}{2m}\nabla^2\psi + V(x)\psi = \mathrm{i}\hbar\frac{\partial\psi}{\partial t}\,. \tag{22}$$

The resulting $O(\hbar^0)$ equation is the Hamilton–Jacobi equation of classical physics,

$$\frac{1}{2m}\left(\nabla S(\mathbf{x})\right)^2 + V(x) = -\frac{\partial S(\mathbf{x})}{\partial t}, \tag{23}$$

whose solution, the action $S(\mathbf{x})$, is the phase of the WKB propagator and also the generating function for the Lagrangian manifold corresponding to the classical system [3]:

$$\mathbf{p}(\mathbf{x}) \equiv \mathbf{p}(t,\mathbf{x}) = \nabla S(\mathbf{x}), \qquad \mathbf{p}(0,\mathbf{y}) = -\nabla_{\mathbf{y}} S. \tag{24}$$

The amplitude of the propagator is the solution to the $O(\hbar)$ equation resulting from (21),

$$A(\mathbf{x})\nabla^2 S(\mathbf{x}) + 2\nabla S(\mathbf{x})\cdot\nabla A(\mathbf{x}) = -\frac{\partial A(\mathbf{x})}{\partial t}\,. \tag{25}$$

The quantity $\rho(\mathbf{x}) \equiv |A(\mathbf{x})|^2$ is interpreted as the probability density associated with an ensemble of classical particles. The initial amplitude, $\rho_0(\mathbf{x})$, (i.e., the amplitude corresponding to $t \to s = 0$, $\mathbf{x} \to \mathbf{y}$) should agree with the correct initial form of the quantum propagator, and the evolution of $\rho(\mathbf{x})$ obeys

$$m\,\frac{\partial\rho\,(\mathbf{x})}{\partial t} = -\nabla\cdot\left[\rho\,(\mathbf{x})\;\mathbf{p}\,(\mathbf{x})\right]\,, \tag{26}$$

where the first of equations (24) defines the momentum field, $\mathbf{p}\,(\mathbf{x})$. Equation (26) is a continuity equation for the probability density function, and it can be shown that the evolution of the density function from the initial configuration, $\mathbf{x}_0 \equiv \mathbf{y}$, to the final configuration, $\mathbf{x}$, is

$$\rho_0(\mathbf{x}_0)\,\mathrm{d}\mathbf{x}_0 = \rho(\mathbf{x})\,\mathrm{d}\mathbf{x} \;\Rightarrow\; \rho(\mathbf{x}) = \rho_o(\mathbf{x}_0)\left|\frac{\partial\mathbf{x}_0}{\partial\mathbf{x}}\right|\,. \tag{27}$$

In the 1-dimensional case the Jacobian $\frac{\partial\mathbf{x}_o}{\partial\mathbf{x}}$ becomes $\frac{\partial y}{\partial x}$.

For the propagator based on trajectories with fixed initial position y, equation (27) becomes inapplicable; the trajectories are labeled by their initial momenta, $p \equiv p(0) \equiv p(0,x)$, and the Jacobian must be replaced by

$$\left|\frac{\partial p}{\partial x}\right| = \left|\frac{\partial^2 S}{\partial x\,\partial y}\right| = \left|\frac{\partial p(t)}{\partial y}\right|, \tag{28}$$

where (24) has been used. In that situation the second of equations (24) is replaced by

$$y = \frac{\partial S}{\partial p}\,. \tag{29}$$

This paper will not consider solutions of (21) higher than $O(\hbar)$. The WKB approximation for the propagator to first order in $\hbar$ is therefore

$$U(\mathbf{x}) = A(\mathbf{x})\,\mathrm{e}^{\frac{\mathrm{i}}{\hbar}S(\mathbf{x})}\,, \tag{30}$$

and is subject to the same initial conditions as the corresponding quantum propagator. For trajectories with initial position data the initial value is (in dimension 1)

$$\lim_{t\to s} U(x) = \delta(x-y)\,, \tag{31}$$

and for trajectories described with initial momentum data the initial value of the propagator is

$$\lim_{t\to s} U(p) = \frac{\mathrm{e}^{\frac{\mathrm{i}}{\hbar}xp}}{\sqrt{2\pi\hbar}}\,. \tag{32}$$

It is often said that the WKB approximation is exact whenever the Hamiltonian is a polynomial of degree at most 2 in both position and momentum. That statement is true, however, only for the propagator, not for solutions of the Schrödinger equation with more general initial data [17], and only when the Hamiltonian is globally of such a form. In our problem we shall find in section 2 that the WKB solution is exact until the wave hits the ceiling but has only $O(\hbar)$ accuracy for the reflected wave.

2. The propagator for initial position data

Throughout this section

$$\mathbf{d}_y \equiv [(y,0),(x,t)]\,, \quad \mathbf{b}_y \equiv [(y,0),(0,b_y)]\,, \quad \mathbf{r}_y \equiv [(0,b_y),(x,t)]\,. \tag{33}$$

Here b_y denotes the time of bounce for a trajectory starting at y. In our considerations x, y, and t are all nonnegative.

The general trajectory and momentum connecting the initial data (y,s) to the final data (x,t) for a linear potential are

$$q(\tau;\mathbf{x}_y) = (\tau-s)^2 + (\tau-s)\left[\frac{x-y}{t-s} - (t-s)\right] + y, \tag{34a}$$

$$p(\tau;\mathbf{x}_y) = (\tau-s) + \frac{1}{2}\left[\frac{x-y}{t-s} - (t-s)\right]. \tag{34b}$$

For the direct paths, $s=0$ in $\mathbf{x}_y$, and the trajectory and momentum are

$$q(\tau;\mathbf{d}_y) = \tau^2 + \tau\left[\frac{x-y}{t} - t\right] + y, \tag{35}$$

$$p(\tau;\mathbf{d}_y) = \tau + \frac{1}{2}\left(\frac{x-y}{t} - t\right). \tag{36}$$

Note that equation (36) implies that a trajectory with initial momentum 0 will have initial position $\tilde{y}$, as predicted (8). Using equations (10), (36), and (35), one sees that the time at which the particle turns around, $n(x, y, t)$, is

$$n = -p = -\left(\frac{x-y}{2t} - \frac{t}{2}\right) = \frac{1}{2}\left(\frac{y-x}{t} + t\right), \tag{37}$$

and the place where this event occurs is

$$q(n) = -\frac{1}{4}\left(\frac{x-y}{t} - t\right)^2 + y. \tag{38}$$

2.1. Admissible paths

In our system the path (35) is admissible if and only if it does not penetrate the ceiling during the time interval $(0, t)$. If $n \leq 0$, the path is admissible and of type (i); if $n \geq t$, it is admissible and of type (ii). If $0 < n < t$ and $q(n) \geq 0$, the path is admissible and of type (iii); if

$$0 < n < t \quad \text{and} \quad q(n) < 0, \tag{39}$$

it is forbidden. After some calculation these two conditions respectively translate to

$$t^2 > |x - y|, \tag{40}$$

$$(x + y - t^2)^2 > 4xy. \tag{41}$$

The solution of (41) falls naturally into two cases: If $t^2 > x + y$, then (41) is equivalent to $t > \sqrt{x} + \sqrt{y}$, and (40) is then satisfied. Conversely, if $t \leq \sqrt{x} + \sqrt{y}$ and $t^2 > x + y$, then $q(n) \geq 0$ and the trajectory is allowed. If $t^2 \leq x + y$, (41) is equivalent to $t^2 \leq |\sqrt{x} - \sqrt{y}|^2$, which is easily shown to contradict (40); so all trajectories are allowed in this case.

In summary, all allowed trajectories satisfy

$$t \leq \sqrt{x} + \sqrt{y} \tag{42}$$

and all forbidden trajectories violate it, in accordance with the energy argument at the end of section 1.2. In the next subsection we verify that (42) is also the necessary and sufficient condition for existence of a bounce trajectory. For given data (y, x, t), therefore, there will be either one direct path and one bounce path, or no path at all. The only exception is the critical case (12), for which the direct and bounce paths are the same.

A finer classification of paths is given in Table 1, which is useful for comparison with the listing of paths of prescribed initial momentum in Table 2 in section 4. Our tables do not include paths corresponding to endpoints of the parameter intervals listed, partly because the classification of those can be ambivalent. The classification is more symmetrical in x and y than it may appear: Interchanging x with y interchanges type (i) with type (ii), and it leaves the type-(iii) region, as a whole, invariant, its boundaries being the lines $t^2 = |x - y|$ and a segment of the parabola $(x - y)^2 - 2(x + y)t^2 + t^4 = 0$.

Table 1. Constraints on the initial position given the final data (x,t). Endpoint cases are not included.

$x\in$	$y\in$	Trajectory
$\left(t^2,\infty\right)$	$\left(0,x-t^2\right)$	Type (i) (rightward)
$(0,\infty)$	$\left(x+t^2,\infty\right)$	Type (ii) (leftward)
$\left(0,t^2\right)$	$\left(\left(\sqrt{x}-t\right)^2,x+t^2\right)$	Type (iii) (turning)
$\left(t^2,\infty\right)$	$\left(x-t^2,x+t^2\right)$	Type (iii) (turning)
$(0,\infty)$	$\left(\left(t-\sqrt{x}\right)^2,\infty\right)$	Bounce

2.2. The time of bounce

From equations (34b) and (34a) the trajectories and momenta for the bounce paths are

$$q_1(\tau;\mathbf{b}_y)=\tau^2-\tau\left(b+\frac{y}{b}\right)+y, \tag{43a}$$

$$q_2(\tau;\mathbf{r}_y)=\left(\tau^2-t^2\right)+\frac{\tau-t}{b-t}\left(-\left(b^2-t^2\right)-x\right)+x, \tag{43b}$$

$$p_1(\tau;\mathbf{b}_y)=\tau-\left(\frac{y}{2b}+\frac{b}{2}\right), \tag{43c}$$

$$p_2(\tau;\mathbf{r}_y)=\tau-\frac{1}{2}\left(\frac{x}{b-t}+(b+t)\right). \tag{43d}$$

Thus the ceiling condition for the bounce trajectory, $q_1(b)=-q_2(b)$, yields the equation

$$f(b)\equiv b^3+a_2b^2+a_1b+a_0=0, \tag{44}$$

$$a_2\equiv-\frac{3t}{2}\,,\quad a_1\equiv\frac{t^2}{2}-\frac{1}{2}\,(x+y)\,,\quad a_0\equiv\frac{yt}{2}\,.$$

The polynomial discriminant of the cubic equation, D, is defined as [18]

$$\begin{aligned}D&\equiv R^2+Q^3 \qquad (45)\\ &=\frac{t^2}{64}\left((x-y)^2-\frac{4}{9}(x+y)^2\right)-\left(\frac{t^2}{12}\right)^3-\left(\frac{1}{6}(x+y)\right)^3-\frac{t^4}{288}(x+y),\end{aligned}$$

where the definitions of R and Q are

$$Q=\frac{3a_1-a_2^2}{9}=-\frac{t^2}{12}-\frac{1}{6}(x+y), \tag{46a}$$

$$R=\frac{9a_1a_2-27a_0-2a_2^3}{54}=\frac{t}{8}(x-y). \tag{46b}$$

If $D>0$ then one root is real and the other two are complex conjugates; $D=0$ if all roots are real and at least two are equal; and $D<0$ if all roots are real and unequal. From equation (45),

$$D(0)<0\qquad\text{and}\qquad\lim_{t\to\infty}D(t)=-\infty. \tag{47}$$

To analyze the discriminant's behavior as $t\to\infty$ let $T\equiv t^2$; then

$$\frac{dD}{dT}=\frac{1}{64}\left((x-y)^2-\frac{4}{9}\,(x+y)^2\right)-\left(\frac{T}{24}\right)^2-\frac{T}{144}\,(x+y)\,. \tag{48}$$

Therefore, the derivative of the discriminant will tend to $-\infty$ as $t \to \infty$. Setting (48) to zero reveals that the critical points of the discriminant occur where

$$t = \pm\sqrt{(x(-2 \pm 3) - y(2 \pm 3))}. \tag{49}$$

The two negative roots are not physical, so the only possible critical points are

$$t_{c+} = \sqrt{x - 5y}, \qquad t_{c-} = \sqrt{y - 5x}. \tag{50}$$

If the initial and final data do not satisfy $x > 5y$ or $y > 5x$, then the derivative of the discriminant will always be negative, and by (47) so will the discriminant. If one of these inequalities is satisfied, then only one of the roots (50) will be real. Without loss of generality, assume $x > 5y$, so that the relevant root of is t_{c+}. Furthermore, relations (47) imply that this root must be a maximum for $D(t)$. Therefore, if $D(t_{c+}) < 0$, then the discriminant will be negative for all values of t. According to (45),

$$D(t_{c+}) = \frac{1}{64}\left((x - 5y)(x - y)^2 - (x - y)^3\right).$$

Thus the discriminant will always be negative if $x - 5y < x - y$, or $y > 0$. Therefore, provided that $y \neq 0$, $D(t) < 0$ for all t and all three roots to equation (44) are real and unequal. Similarly, if $y > 5x$ then the requirement that $D(t) < 0$ is $x > 0$, which is in general true except for the special case $x = 0$. The special cases $y = 0$ and $x = 0$ respectively imply that the initial and final positions are at the ceiling; the respective times of bounce are 0 and t.

The maximum and minimum of the cubic function (44) are

$$b_{c\pm} = \frac{t}{2} \pm \sqrt{\frac{t^2}{12} + \frac{1}{6}(x + y)},$$

and the point at which the equation changes its concavity is $\frac{t}{2}$. Since $b \to \pm\infty$ implies $f(b) \to \pm\infty$, the point b_c is where $f(b)$ changes from concave to convex. Since all three roots must be real, one root of $f(b)$ will lie between the two extrema, and the other two must lie outside of the range:

$$r_1 \in (-\infty, b_{c-}), \qquad r_2 \in (b_{c+}, \infty), \qquad r_3 \in (b_{c-}, b_{c+}). \tag{51}$$

Since r_3 is the only root which may equal t and 0, which are the critical values of the bounce time, and the bounce time is a continuous function, r_3 is the correct root for all trajectories. Therefore, if a root of $f(b)$ is found which agrees with the critical trajectories, it will be the correct root for all the trajectories.

For the case where $D < 0$ the three cubic roots may be written as (e.g., [18, 19])

$$r_j(x, y, t) = \frac{t}{2} + 2\sqrt{-Q(x, y, t)}\cos\left(\frac{\Theta(x, y, t) + 2j\pi}{3}\right), \tag{52}$$

where $j = 0, 1, 2$ and

$$\Theta(x, y, t) = \arccos\left(\frac{R(x, y, t)}{\sqrt{-Q(x, y, t)^3}}\right). \tag{53}$$

Finally, for a trajectory in which $x = y$, the correct bounce time is $b_y = \frac{t}{2}$, and only the last range in (52) contains this value. Therefore, by the considerations above

$$\begin{aligned} b_y &= r_2(x, y, t) \\ &= \frac{t}{2} + \frac{1}{\sqrt{3}}\sqrt{t^2 + 2(x+y)}\sin\left[\frac{1}{3}\,\sin^{-1}\frac{3\sqrt{3}\,t(y-x)}{(t^2+2(x+y))^{3/2}}\right]. \end{aligned} \tag{54}$$

2.3. The action

To complete the WKB construction the action of the trajectories and the amplitude function must be determined. From equations (34a) and (34b) the general Lagrangian for the initial-position formulation is

$$\begin{aligned} L\left[q, \dot{q}, \tau\right] &= p(\tau; \mathbf{x}_y)^2 + q(\tau; \mathbf{x}_y) \\ &= 2\left(\tau - t_0\right)^2 + 2\left(\tau - t_0\right)\left[\frac{x-y}{t-t_0} - (t - t_0)\right] + \frac{1}{4}\left[\frac{x-y}{t-t_0} - (t-t_0)\right]^2 + y, \end{aligned} \tag{55}$$

and the corresponding action is

$$\begin{aligned} S_y(t; \mathbf{x}_y) = \frac{2}{3}\left(t - t_0\right)^3 &+ \left(t - t_0\right)^2\left[\frac{x-y}{t-t_0} - (t-t_0)\right] \\ &+ (t - t_0)\left(\frac{1}{4}\left[\frac{x-y}{t-t_0} - (t-t_0)\right]^2 + y\right). \end{aligned} \tag{56}$$

Therefore, the actions for the direct and bounce trajectories are

$$S_{\mathbf{d}y} = S_y(t; \mathbf{d}_y), \tag{57a}$$

$$S_{\mathbf{b}y} = S_y(b_y; \mathbf{b}_y) + S_y(t; \mathbf{r}_y). \tag{57b}$$

Note that for the direct case, as $t \to 0$ the action becomes

$$\lim_{t\to 0} S_y(t; \mathbf{d}_y) \to \ frac(x-y)^2 4t\,, \tag{58}$$

which is the free particle action.

2.4. The amplitude

From equations (36) and (28), the amplitude for the direct trajectory is

$$\sqrt{\frac{1}{2\pi \mathrm{i}}}\sqrt{\frac{\partial p(t; \mathbf{d}_y)}{\partial y}} = \frac{1}{\sqrt{4\pi \mathrm{i} t}}\,. \tag{59}$$

Note that as $(x, t) \to (x, 0)$ the constructed amplitude yields the correct initial condition, $\delta\left(y - x\right)$:

$$\lim_{t\to 0}\frac{1}{\sqrt{4\pi \mathrm{i} t}}\,e^{\mathrm{i}S_d(x,y,t)} = \lim_{t\to 0}\frac{1}{\sqrt{4\pi \mathrm{i} t}} e^{\frac{(y-x)^2}{4\mathrm{i}t}} = \delta\left(y - x\right)\,.$$

Using r_2 from equation (52) and $p_1(0)$ from equation (43c), we find the Jacobian corresponding to the action for the bounce case:

$$\begin{aligned}\frac{\partial p(0;\mathbf{b}_y)}{\partial x} &= \left(\frac{y}{2b_y^2}-\frac{1}{2}\right)\frac{\partial b_y}{\partial x}\\ &= \left(\frac{y}{2b_y^2}-\frac{1}{2}\right)\frac{\cos\left(\frac{\Theta+4\pi}{3}\right)}{6\sqrt{-Q}}\left[1-\frac{Q}{6\sqrt{-D}}\left(\frac{t}{2}+\frac{R}{Q^4}\right)\tan\left(\frac{\Theta+4\pi}{3}\right)\right].\end{aligned} \tag{60}$$

However, linearizing the classical equations of motion for the potential $V=-|q|$, and then "folding" the negative half of the plane onto the positive half produces a more explicit form of the Jacobian. For the given potential we have

$$-\frac{\partial V}{\partial q}=\mathrm{sgn}(q)=2\theta(q)-1, \tag{61}$$

where $\theta(q)$ is the Heavyside step function. Differentiating (61) with respect to a parameter, α, yields

$$\frac{\partial}{\partial\alpha}\left[2\theta(q)-1\right]=2\delta(q)=2\,\frac{\delta(\tau-b_y)}{|\dot q(b_y)|}\,\frac{\partial q}{\partial\alpha}\,. \tag{62}$$

where we have used the functional dependence of the trajectory $q(\tau)$ and the fact that $q(b_y)=0$. Using equation (43c) and the fact that $p(b_y)<0$ for the trajectory moving toward the ceiling, we have

$$|\dot q(b_y)|=\frac{y}{b_y}-b_y\,. \tag{63}$$

Therefore, differentiating Hamilton's equations with respect $\alpha\equiv y$ yields

$$\frac{\mathrm{d}}{\mathrm{d}\tau}\frac{\partial p}{\partial y}=2\,\frac{\delta(\tau-b_y)}{|\dot q(b_y)|}\frac{\partial q}{\partial y}\,, \tag{64a}$$

$$\frac{\mathrm{d}}{\mathrm{d}\tau}\frac{\partial q}{\partial y}=2\frac{\partial p}{\partial y}\,. \tag{64b}$$

For the trajectory moving toward the ceiling, $\tau<b_y$, equation (64a) predicts

$$\frac{\mathrm{d}}{\mathrm{d}\tau}\frac{\partial p}{\partial y}=0,$$

so that $\frac{\partial p}{\partial y}$ is a constant. Therefore,

$$\frac{\partial p}{\partial y}(\tau)=C\equiv\frac{\partial p}{\partial y}(0) \tag{65}$$

for $\tau<b_y$, and hence the solution to (61) for $\tau<b_y$ is

$$\frac{\partial q}{\partial y}=2C\tau+1, \tag{66}$$

since $q(0)=y$ implies $\frac{\partial q}{\partial y}(0)=1$. Integrating (64$a$) for $\tau>b_y$ and using equation (63) yields

$$\frac{\partial p}{\partial y}=C+\frac{2}{|\dot q(b_y)|}\frac{\partial q}{\partial y}(b_y)=\frac{C\left[y+3b_y^2\right]+2b_y}{y-b_y^2}\,. \tag{67}$$

And using this result for $\frac{\partial q}{\partial y}$ yields

$$\frac{\partial q}{\partial y}(\tau) = \frac{\partial q}{\partial y}(b_y) + 2\frac{\partial p}{\partial y}\int_{b_y}^{t} d\tau = \frac{\partial q}{\partial y}(b_y) + 2\frac{\partial p}{\partial y}\left(\tau - b_y\right).$$

Since $q(t) = x$ it follows that $\frac{\partial q}{\partial y}(t) = 0$. Therefore, after algebraic manipulations, the constant C is

$$\frac{\partial p}{\partial y}(0) = \frac{1}{2}\,\frac{5b_y^2 - 4tb_y - y}{\left(y - b_y^2\right)b + \left(t - b_y\right)\left(y + 3b_y^2\right)}\,. \tag{68}$$

Finally, putting this result into (67) and using the cubic equation to simplify the denominator, we get the desired Jacobian:

$$-\frac{\partial p}{\partial y}(t) = \frac{b_y^2 - y}{2\left[-3tb_y^2 + 2(t^2 - x - y)b_y + 3yt\right]}\,; \tag{69}$$

the minus sign comes from "folding" the negative half-plane over.

The initial amplitude function for the bounce trajectories must match in magnitude the one for the direct trajectories, (59). Therefore, the final form of the amplitude function for bounce paths is, up to a possible phase,

$$A_{yb} = \frac{1}{\sqrt{2\pi\mathrm{i}}}\left|\frac{b_y^2 - y}{2\left[-3tb_y^2 + 2(t^2 - x - y)b_y + 3yt\right]}\right|^{\frac{1}{2}}. \tag{70}$$

Equation (12) predicts that on the critical curve, $x = t^2 + y - 2t\sqrt{y}$. Since the critical curve for the bounce path is identical with the trajectory of type (iii) for $E = 0$, the time of bounce is given by n_y on the critical curve. And substituting for x into equation (37) yields

$$y = b_y^2 \tag{71}$$

on the critical curve. Therefore, the amplitude for the bounce path will vanish on the critical curve. Below the critical curve (in the "allowed" region) $y > b_y^2$, so the numerator in (70) is negative.

On the ceiling we want the bounce propagator to agree numerically (up to sign, see below) with the direct propagator of which it is a continuation. This limit corresponds to $x = 0$ and $b_y = t$. One can check (see (72a) and (72b) below) that the actions agree there, and that the denominator in the bounce amplitude reduces as

$$-3tb_y^2 + 2(t^2 - x - y)b_y + 3yt = -3t^3 + 2t^4 - 2yt + 3yt = t(y - b_y^2),$$

so that the amplitudes match as well.

Putting everything together we have the WKB propagators for the direct and bounce cases:

$$U_{y\mathrm{d}}(x, y, t) = \frac{1}{\sqrt{4\pi\mathrm{i}t}}\exp\left[\mathrm{i}\left(\frac{2}{3}t^3 + t^2\left[\frac{x - y}{t} - t\right] + t\left(\frac{1}{4}\left[\frac{x - y}{t} - t\right]^2 + y\right)\right)\right], \tag{72a}$$

$$U_{y\mathrm{b}}\,(x, y, t) = \frac{1}{\sqrt{4\pi\mathrm{i}}}\left[\frac{y - b_y^2}{-3tb_y^2 + 2(t^2 - x - y)b_y + 3yt}\right]^{\frac{1}{2}}$$

$$\times \exp\left[\mathrm{i}\left(\frac{2}{3}b_y^3 - b_y^2\left[\frac{y}{t}+b\right] + b\left(\frac{1}{4}\left[\frac{y}{t}+b_y\right]^2 + y\right)\right)\right]$$
$$\times \exp\left[\mathrm{i}\left(\frac{2}{3}(t-b_y)^3 + (t-b_y)^2\left[\frac{x}{t}-(t-b_y)\right]\right)\right]$$
$$\times \exp\left[\mathrm{i}\,\frac{(t-b_y)}{4}\left(\frac{x}{t}-(t-b_y)\right)^2\right]. \qquad (72b)$$

Note that, with the exception of the constraints on the initial position, the propagator for the direct paths is identical with that for the linear potential without a ceiling, as given in (19). The complete propagator obeying the Dirichlet boundary condition, $\psi(0,t)=0$, must vanish at the ceiling. Therefore, its correct WKB approximation is the *difference*, $U_{y\mathrm{d}} - U_{y\mathrm{b}}$, if the phase convention for the bounce propagator is that adopted in (72*b*). The *sum* solves, to lowest order in $\hbar$, the Neumann problem, $\frac{\partial\psi(0,t)}{\partial x}=0$ (by virtue of (24) and (5)). (In more technical language, (72*b*) does not include the Maslov index, or, rather, its analogue for a sharp boundary.)

3. Soft ceilings

What is happening at the critical curve, $t=\sqrt{x}+\sqrt{y}$, is made clearer by studying a smoother model. We replace the hard ceiling (Dirichlet boundary condition) by a smooth but steeply rising potential. For algebraic convenience we place the ceiling at $x=1$ and the barrier on the right instead of the left; then the potential function

$$V(x) = x + x^n \qquad (73)$$

for some large n does what we want. We take n to be an even integer. Then as $n\to+\infty$, the term x^n vanishes for $|x|<1$ and approaches infinity for $|x|>1$. The barrier at $x=-1$ was not present in our original scenario (where it would have been at $x=2$), but it will not affect the classical solutions in the regime where we shall examine them.

A potential of this type creates a conventional caustic to which the Maslov theory applies. As $n\to\infty$, part of the caustic curve converges to the critical curve while the rest of the caustic converges to the initial portion of the ceiling. The families of classical trajectories starting from $y=0$ are displayed by *Mathematica* in Figures 4 and 5 for $n=6$ and 30, respectively. The stray curves in the upper right of the closeup plots, 4(b) and 5(b), are artifacts of instability in the numerical solution of the differential equation; it is not surprising that these occurred very close to the caustic limit where various solutions are nearly tangent. (The physical invalidity of these curves is clear from the observation that they intersect other trajectories that started with greater kinetic energy but now appear to have less.) The returning trajectories in the lower right of plots 4(a) and 5(a), on the other hand, are artifacts of the model, representing reflection off the gratuitous floor at $x=-1$ introduced by the potential (73).

Disregarding these extraneous features, one clearly sees a standard fold caustic, the envelope of the trajectories, developing at the top of the figures. Below the caustic each point has two trajectories through it, which we can label "bounce" or "direct" according

Figure 4. A family of paths leaving the origin with various initial momenta, for $n = 6$ in (73). Formation of a fold caustic at the top of the figure is clearly visible. Horizontal axis is t, vertical is x, y is fixed.

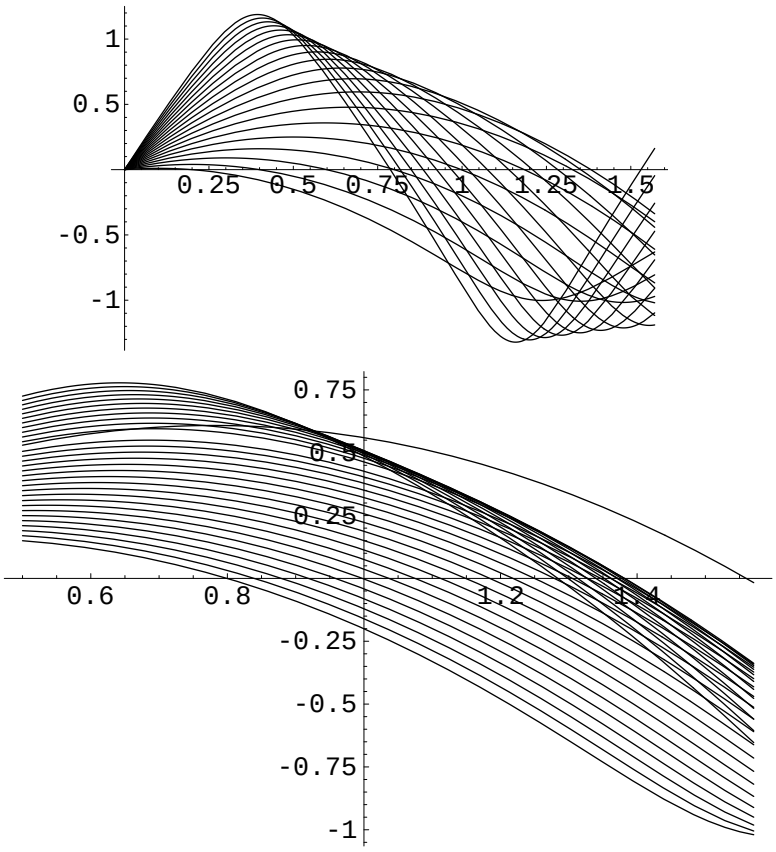

to whether or not the path is returning from touching the caustic. For a fixed y, all sufficiently energetic paths appear, for large n, to bounce off the horizontal line $x = 1$, which becomes the ceiling. Less energetic paths do not reach all the way to the ceiling, but on their return they cross over paths of still lower energy, creating an envelope close to the critical trajectory of the hard-ceiling problem.

If we were to construct the semiclassical propagator for this system, we would presumably find that it is a poor approximation near the caustic, in the sense that when substituted into the time-dependent Schrödinger equation (13)) it leaves a large residual. At points well inside the caustic ($\sqrt{x} \ll t - \sqrt{y}$) it should be a good approximation if direct and bounce contributions are combined with the proper phase. Nevertheless, as $n \to \infty$ the contribution of the direct paths alone will converge to $U_{\rm yd}$ in (72a), which we have seen to be an exact solution of (13) (though not of the ceiling boundary condition). That is, the region where $U_{\rm yd}$ is a poor solution is pressed into the caustic boundary as $n \to \infty$, as (73) increasingly well approximates a pure linear potential at smaller x.

Near a typical caustic the amplitude function (28) of the semiclassical approximation diverges, since it is the Jacobian determinant of the mapping from initial momentum to final position (which is by definition singular on the caustic).

Figure 5. The same for $n = 30$. The leftmost part of the caustic curve is converging to a "ceiling" at $x = 1$. The trajectory in the upper right is close to the critical trajectory (12) and can be loosely described as "the last path that misses the caustic".

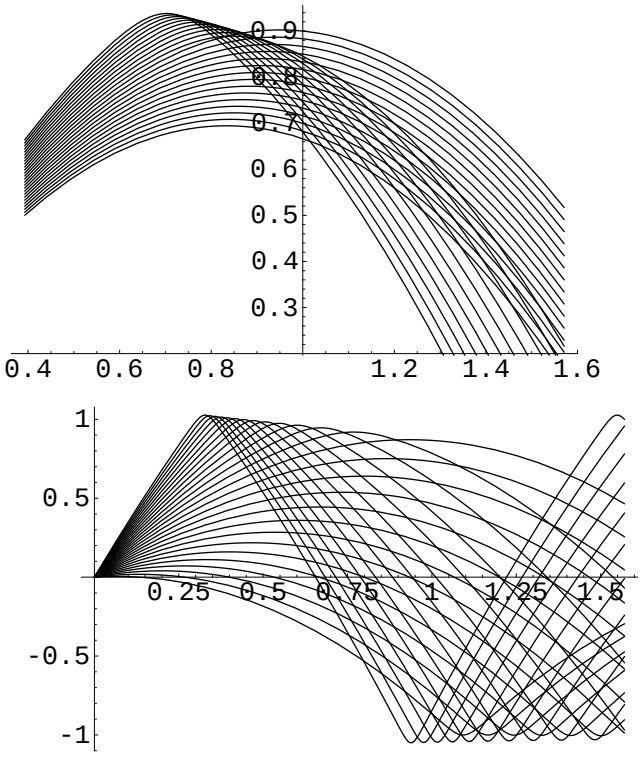

As just remarked, this is not true of the semiclassical solution for the hard wall, (72a) and (72b). The amplitude of (72b) actually vanishes on the critical curve. It does, however, have a square-root singularity there, so that its residual in (13) (which involves second derivatives of the amplitude) will still blow up. For this reason, and because the position-space semiclassical construction yields no nonzero prediction at all for the region of space-time beyond the caustic, we turn in the next section to a momentum-space construction.

4. The propagator for initial momentum data

Throughout this section the denotation of initial data, (p, s), and final data, (x, t), is

$$\begin{aligned}
\mathbf{d}_p &\equiv [(p, 0), (x, t)]\,, \\
\mathbf{b}_p &\equiv [(p, 0), (0, b_p)]\,, \\
\mathbf{r}_p &\equiv [(-p - b_p, b_p), (x, t)]\,.
\end{aligned}$$

The general classical path and the corresponding momentum connecting the initial data (p, s) with final data (x, t) are

$$q(\tau; \mathbf{x}_p) = (\tau - t)^2 + 2\,(\tau - t)\,(p + t - s) + x \tag{74a}$$

$$p(\tau; \mathbf{x}_p) = (\tau - s) + p. \tag{74b}$$

The general Hamiltonian of the classical system is therefore

$$H(\tau;\mathbf{x}_p) = (t-s+p)^2 - x. \tag{75}$$

Setting $s=0$ corresponds to the direct paths under consideration in this paper, and to the initial segments of bounce paths:

$$q(\tau;\mathbf{d}_p) = (\tau-t)^2 + 2(\tau-t)(p+t) + x, \tag{76a}$$

$$p(\tau;\mathbf{d}_p) = \tau + p. \tag{76b}$$

The Hamiltonian for the direct case is therefore given by

$$H_{p,d} = (p+t)^2 - x = p^2 + 2pt + t^2 - x, \tag{77}$$

and the energy of the trajectory may therefore be categorized by:

$$H_{p,d} > 0: \quad p \in \left(-\infty, -\sqrt{x}-t\right) \cup \left(\sqrt{x}-t, \infty\right), \tag{78a}$$

$$H_{p,d} = 0: \quad p = \pm\sqrt{x} - t, \tag{78b}$$

$$H_{p,d} < 0: \quad p \in \left(-\sqrt{x}-t, \sqrt{x}-t\right). \tag{78c}$$

Using equation (74*a*), the bounce paths may be characterized as:

$$q(\tau;\mathbf{b}_p) = (\tau-b_p)^2 + 2(\tau-b_p)(p+b_p), \tag{79a}$$

$$q(\tau;\mathbf{r}_p) = (\tau-t)^2 + 2(\tau-t)(t-p-2b_p) + x. \tag{79b}$$

The Hamiltonian for the bounce trajectories is thus

$$H_{p,b} = p(b_p;\mathbf{b}_p)^2 = (p+b_p)^2. \tag{80}$$

Note that the bounce Hamiltonian is always greater than or equal to zero, with equality for $p=-b_p$.

Since all trajectories are required to stay on the positive side of the ceiling, the initial momentum for the non-bounce trajectories is constrained by

$$q(0;\mathbf{d}_p) = -t^2 - 2pt + x \geq 0.$$

Therefore a constraint on type (i) and types (ii) and (iii) trajectories is, respectively,

$$0 < p \leq \frac{x}{2t} - \frac{t}{2}, \tag{81}$$

$$p \leq \frac{x}{2t} - \frac{t}{2} < 0. \tag{82}$$

4.1. Trajectories of type (i)

For the particle to initially move away from the ceiling, $p>0$. Equation (81) is the only other constraint on the system and therefore specifies the interval of integration over p for this class of paths. Note that (81) implies $\sqrt{x} > t$; therefore, since $\sqrt{x}-t < \frac{x-t^2}{2t}$, equations (78*a*) and (78*c*) imply that the energy of type (i) trajectories may be either greater than or less than zero:

$$H<0: \quad p \in \left(0, \sqrt{x}-t\right)$$

$$H>0: \quad p \in \left(\sqrt{x}-t, \frac{x-t^2}{2t}\right).$$

4.2. Trajectories of type (ii)

Besides the requirement that $p < 0$, and equation (82), the particle must also not turn around nor enter the forbidden region. Equation (76b) shows that a turning point of the trajectory will occur at $\tau = -p = |p|$, therefore $t < |p|$. Forbidding the particle to turn around and requiring $x > 0$ are enough to ensure that the trajectory will not enter the forbidden region. Since $-t < \frac{x}{2t} - \frac{t}{2}$, the second constraint is weaker than the first and hence the operative constraint on the initial momentum is

$$p < -t \tag{83}$$

for trajectories of type (ii).

Finally, equations (78a) and (78c) reveal that the energy of the trajectory may again be greater than or less than zero according to:

$$\begin{aligned} H_{p,d} > 0: &\quad p \in \left(-\infty, -\sqrt{x} - t\right), \\ H_{p,d} < 0: &\quad p \in \left(-\sqrt{x} - t, -t\right). \end{aligned} \tag{84}$$

4.3. Trajectories of type (iii)

Using equations (10) and (77), the position and energy of the particle at the turning point are

$$q(n; \mathbf{d}_p) = x - (p + t)^2 = -H_{p,d}. \tag{85}$$

Therefore, a turning-point trajectory implies that the energy is less than zero; otherwise the turning point is behind the ceiling. Using equation (78c), the initial momentum is therefore constrained by:

$$-\sqrt{x} - t < p < \sqrt{x} - t.$$

Also, the opposite of equation (83) must be true; otherwise the turning point would not have time to occur:

$$t > |p| \Rightarrow p > -t. \tag{86}$$

If $\sqrt{x} > t \Rightarrow x > t^2$, then the upper bound in equation (78c) will be positive. Therefore, the regions corresponding to the momentum of the particle and the energy being less than zero are:

$$\begin{aligned} x < t^2: &\quad p \in \left(-\sqrt{x} - t, \sqrt{x} - t\right) \\ x > t^2: &\quad p \in \left(-\sqrt{x} - t, 0\right). \end{aligned}$$

However, equation (86) implies that the lower bounds must be replaced by $-t$, therefore the correct constraints on the momentum are:

$$x < t^2: \quad p \in \left(-t, \sqrt{x} - t\right), \tag{87a}$$

$$x > t^2: \quad p \in (-t, 0). \tag{87b}$$

4.4. Bounce trajectories

Since the construction of equations (74b), (79a), and (79b) guarantees the validity of (5), the final constraint to impose on the bounce trajectories is the location of the ceiling:

$$q(b_p; \mathbf{r}_p) = 0. \tag{88}$$

This yields the quadratic equation

$$b_p^2 + b_p \left(\frac{2}{3}p - \frac{4}{3}t\right) + \frac{1}{3}\left(t^2 - 2pt - x\right) = 0,$$

with solution

$$b_p = \frac{1}{3}\left(2t - p \pm \sqrt{(p+t)^2 + 3x}\right).$$

Requiring the time of bounce, b_p, to be less than the trajectory time, t, and the initial momentum to be less than zero yields

$$(|p| - t) \pm \sqrt{(|p| - t)^2 + 3x} \leq 0, \tag{89}$$

which requires the negative root. Therefore, independently of the relationship between the initial momentum and the trajectory time, the correct bounce time is given by

$$b_p = \frac{1}{3}\left(2t - p - \sqrt{(p+t)^2 + 3x}\right). \tag{90}$$

Constraining the initial position of the trajectory to be in the classical region implies

$$q(0; \mathbf{b}_p) > 0 \Rightarrow 0 < b_p < -2p. \tag{91}$$

However, the "critical" trajectory for the bounce path is when the initial momentum is equal to the time of bounce, which corresponds to the particle just grazing the ceiling. All other initial momenta must be greater, in magnitude, than the time of bounce:

$$0 < b_p < -p. \tag{92}$$

This constraint is stronger than (91) and therefore is the final constraint to impose on the bounce trajectories. Equality on the right side of (92) implies

$$2t + 2p - \sqrt{(t+p)^2 + 3x} = 0. \tag{93}$$

This leads, on the one hand, to

$$p = -t \pm \sqrt{x}. \tag{94}$$

But now (93) also requires that $t + p > 0$, so the correct solution is

$$p = \sqrt{x} - t. \tag{95}$$

On the other hand, the initial momentum corresponding to a bounce time equal to zero is the solution of

$$2t - p - \sqrt{(t+p)^2 + 3x} = 0,$$

or

$$p = \frac{t^2 - x}{2t}. \tag{96}$$

Table 2. Constraints on the initial momentum given the final data (x,t). Endpoint cases are not included.

$x \in$	$p \in$	Trajectory
(t^2,∞)	$\left(0,\frac{x-t^2}{2t}\right)$	Type (i) (rightward)
$(0,\infty)$	$(-\infty,-t)$	Type (ii) (leftward)
$(0,t^2)$	$(-t,\sqrt{x}-t)$	Type (iii) (turning)
(t^2,∞)	$(-t,0)$	Type (iii) (turning)
$(0,t^2)$	$(-\infty,\sqrt{x}-t)$	Bounce
(t^2,∞)	$\left(-\infty,\frac{t^2-x}{2t}\right)$	Bounce

The right-hand sides of (96) and (95) have opposite signs, and only negative values of them are operative. Therefore, the constraints to impose on the initial momentum so that both inequalities (92) hold are

$$x < t^2: \quad p < \sqrt{x} - t, \tag{97a}$$

$$x > t^2: \quad p < \frac{t^2 - x}{2t}\,. \tag{97b}$$

The constraints on the initial momentum for given final data (x,t) are summarized in Table 2. They are somewhat more complex than those for given initial position in section 2, although in compensation we did not need to solve a cubic equation this time.

If $x \in (t^2,\infty)$, all four types of trajectories may occur for various initial momenta.

If the initial momentum is positive, only the trajectory of type (i) is allowable. Even it does not exist if p is too large for the given (x,t) (or if $x < t^2$).

For $p < 0$, further analysis reveals a distinction between the regions $x \in (t^2, 3t^2)$ and $x \in (3t^2,\infty)$. In both cases the monotonic (type (ii)) and turning regimes of p are mutually exclusive. When $x < 3t^2$, the bounce regime overlaps both of those, but when $x > 3t^2$, the bounce regime is a subset of the monotonic one. In either case there is a possibility of only one path — that is, a bounce path may not exist for the given data.

For $x \in (0,t^2)$ there are no paths corresponding to positive initial momentum. The intervals corresponding to the always left-moving and the turning trajectories are disjoint and their union coincides with the bounce interval. Therefore, two paths are always possible for $x \in (0,t^2)$; one will always be a bounce, and the other is either type (ii) ($p < 0$) or turning.

In short, there are regimes of (p,x,t) data where only one path exists and other regimes where two exist, or none. In contrast, for (y,x,t) data, if a path exists at all (i.e., (42) is satisfied), then there will always be two distinct trajectories, except in the very special case of a critical trajectory.

4.5. The action

Using equations (74a) and (74b), the classical Lagrangian for the general initial and final conditions is found to be

$$L_p(\tau;\mathbf{x}_p) = (\tau - s + p)^2 + (\tau - t)^2 + 2\,(\tau - t)\,(p + t - s) + x. \tag{98}$$

Thus the general action for $\tau = t$ and arbitrary initial and final data, $\mathbf{x}_p$, up to a constant of integration, S_0, is

$$S_p(\mathbf{x}_p) = -\,\frac{(t-s)^3}{3} + (t-s)\left(x + p^2\right) + S_0 = S + S_0\,. \tag{99}$$

The following partial derivatives of the general action will again prove useful in determining the appropriate initial condition:

$$\frac{\partial S}{\partial t}(\mathbf{x}_p) = -\,(t-s)^2 + \left(p^2 + x\right), \tag{100a}$$

$$\frac{\partial S}{\partial s}(\mathbf{x}_P) = (t-s)^2 - \left(p^2 + x\right) = -\,\frac{\partial S}{\partial t}\,, \tag{100b}$$

$$\frac{\partial S_p}{\partial x}(\mathbf{x}_p) = (t-s)\,. \tag{100c}$$

Using the derivatives of the general initial position from equation (74a),

$$\frac{\partial q}{\partial t}(s;\mathbf{x}_p) = -2\,(p + t - s)\,, \tag{101a}$$

$$\frac{\partial q}{\partial x}(s;\mathbf{x}_p) = 1, \tag{101b}$$

one sees that the correct initial action is

$$S_0 = p(s;\mathbf{x}_p)\,q(s;\mathbf{x}_p) = p\,q(s;\mathbf{x}_p),$$

because then (cf. (29))

$$\frac{\partial S_p}{\partial t} = -H(\mathbf{x}_p), \tag{102a}$$

$$\frac{\partial S_p}{\partial x} = p(t;\mathbf{x}_p), \tag{102b}$$

$$\frac{\partial S_p}{\partial p} = q(s;\mathbf{x}_p). \tag{102c}$$

Then the actions for the direct and bounce cases are respectively

$$\begin{aligned} S_{pd} &= S_p(\mathbf{d}_p) + p\,q(0;\mathbf{d}_p) \\ &= -\,\frac{t^3}{3} - p\,t(p+t) + x(p+t), \end{aligned} \tag{103a}$$

$$\begin{aligned} S_{pb} &= S_p(\mathbf{b}_p) + S_p(\mathbf{r}_p) + p\,q(0;\mathbf{b}_p) \\ &= -\,\frac{1}{3}\left[b_p^3 + (t-b_p)^3\right] - b_p p\,(p+b_p) + (t-b_p)\left(x + (p+b_p)^2\right) - p b_p(2p+b_p). \end{aligned} \tag{103b}$$

In these calculations, terms resulting from the differentiation of b_p play a crucial role, whereas in the initial-position formulation they cancel each other.

4.6. The amplitude

The Jacobian corresponding to the amplitude function is $\left|\frac{\partial q(s)}{\partial q(t)}\right|$. Using equation (74$a$) for the trajectories yields for the direct case

$$\frac{\partial q(0)}{\partial x} = 1, \tag{104}$$

which reveals that the amplitude for the direct case is a constant solely depending on the initial density of particles. This initial density must be in agreement with the the initial form of the quantum propagator in the momentum representation, and therefore

$$A_d = \frac{1}{\sqrt{2\pi}}\,. \tag{105}$$

Using equations (79a) and (79b) for the trajectories in the Jacobian for the bounce amplitude yields

$$\frac{\partial q_1(0)}{\partial x} = \frac{p + b_p}{\sqrt{(p+t)^2 + 3x}}\,, \tag{106}$$

and therefore the amplitude function for the bounce trajectory is, up to a phase,

$$A_b = \frac{1}{\sqrt{2\pi}}\sqrt{\left|\frac{p + b_p}{\sqrt{(p+t)^2 + 3x}}\right|}, \tag{107}$$

where the initial (normalization) factor is carried over from the incident direct path.

Since the critical curve for the bounce trajectory is equivalent to the $E = 0$ type-(iii) trajectory, it is evident that $b_p = n_p = -p$ for the critical trajectory. Hence the amplitude will vanish for the critical path. All other values of b_p are less than $-p$, by (92). Therefore, the numerator of equation (107) will be negative for bounce paths. As in section 2, our phase convention is that the direct and bounce propagators agree at the ceiling, $x = 0$. Therefore, the correct bounce amplitude is

$$A_{pb} = \frac{1}{\sqrt{2\pi}}\sqrt{\frac{|p + b_p|}{\sqrt{(p+t)^2 + 3x}}}\,. \tag{108}$$

And, with this convention, to $O(\hbar)$ the WKB approximation for the quantum propagator is the difference, $U_{p\mathrm{d}} - U_{p\mathrm{b}}$. of the propagators constructed from the bounce and non-bounce paths:

$$U_{p\mathrm{d}}(x,p,t) \quad = \frac{1}{\sqrt{2\pi}}\,\exp\left[\mathrm{i}\left(-\frac{t^3}{3} + t\left(p^2 + x\right) - p\left(t^2 + pt - x\right)\right)\right], \tag{109a}$$

$$U_{p\mathrm{b}}(x,p,t) \quad = -\frac{1}{\sqrt{2\pi}}\sqrt{\frac{|p + b_p|}{\sqrt{(p+t)^2 + 3x}}}\,\exp\left[i\left(-\frac{1}{3}\left[b_p^3 + (t - b_p)^3\right] - b_p p\,(3p + 2b_p)\right)\right]$$
$$\times \exp\left[i\left((t - b_p)\left(x + (p + b_p)^2\right)\right)\right]. \tag{109b}$$

Here b_p is defined by (90).

5. Numerical comparison of the propagators

In this section we try out the propagators (109*a*), (109*b*), (72*a*), and (72*b*) by applying them to localized wave packets. We take the initial state of the system in position space to be a general Gaussian wave packet:

$$\psi\,(y) = \left(\frac{2}{\gamma\pi}\right)^{\frac{1}{4}} \mathrm{e}^{-\frac{(y-\bar{y})^2}{\gamma} - \mathrm{i}y\bar{p}}, \tag{110}$$

where y denotes the initial position, the average initial position is $\bar{y}$, the average initial momentum is $\bar{p}$, and the constant γ prescribes the width of the packet. Then the initial wave packet in momentum space is the Fourier transform of (110):

$$\phi\,(p) = \left(\frac{\gamma}{2\pi}\right)^{\frac{1}{4}} \mathrm{e}^{-\gamma\frac{(p+\bar{p})^2}{4} - \mathrm{i}\bar{y}(p+\bar{p})}, \tag{111}$$

which is also Gaussian, with width $4/\gamma$.

Gaussians are chosen to make the treatment as symmetrical as possible between position space and momentum space, thereby minimizing any bias in numerical calculations and their interpretation. Unfortunately, the support of the Gaussian $\psi(y)$ extends into the forbidden region $y < 0$, so it does not represent a state of our system, strictly speaking. A momentum-space counterpart of this fact is that the signed momentum does not exist as a legitimate quantum observable (a self-adjoint operator) when the configuration space is a half-line. An exact Fourier analysis of such a system would require Fourier sine transforms and a "momentum" observable that is nonnegative. However, the whole spirit of the semiclassical approximation requires that the particle be thought of as approximately localized and having an approximate classical momentum, and our foregoing calculations have been conducted in this framework. If

$$\bar{y} \gtrsim \gamma, \tag{112}$$

then we expect the semiclassical picture to hold. Furthermore, because of the rapid decay of the Gaussian function, whenever the wave packet $\psi(y)$ or $\phi(p)$ is located well inside a classically allowed region in the sense of Table 1 or 2, the limits of integration can be extended to infinity without committing great error.

Figure 6 depicts the evolution of an initial Gaussian wave function from an initial time $\tau = 0$ to a final point (x, t). From each initial point to the right of a critical value, y_c, there are two trajectories that arrive at (x, t). The contribution of each path to the wave function at (x, t) is weighted by the initial wave packet and otherwise determined by the propagator (direct or bounce, as appropriate). The value of y_c is determined from (42) to be

$$y_c = (t - \sqrt{x})^2. \tag{113}$$

Note that the roles of x and y in Figures 3 and 6 are reversed, so that in Figure 6 the classically forbidden region is below and to the left of the critical trajectory starting from y_c.

Figure 6. Plot of WKB evolution of an initial wave packet, from the point of view of a final point (x, t) The solid lines are the classical trajectories to that point for a particle initially located at the average value of the initial wave packet; the dashed lines are the classical paths starting at points rather far into the wings of the initial packet. The classically forbidden region for trajectories is at the lower left of the plot, bounded by the critical trajectory (not shown), which intersects the horizontal axis at a point y_c (compare Figure 3, inverted).

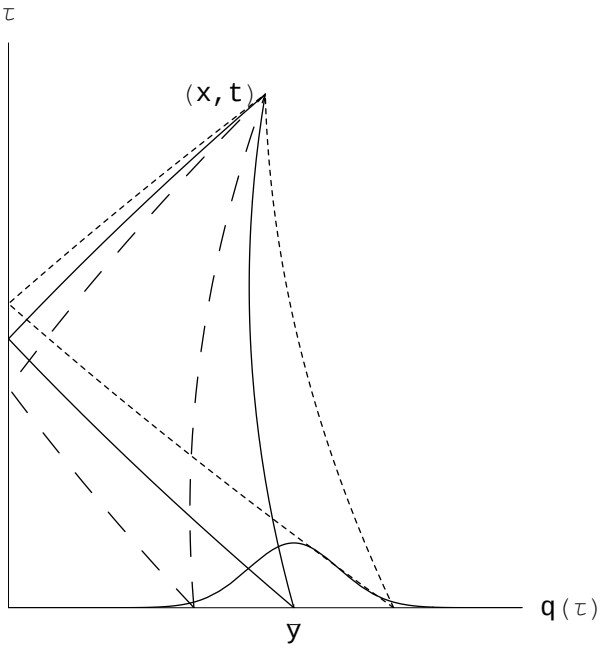

Figures 7 and 8 show the real parts of the direct and bounce contributions to the final wave function at the point $(x, t) = (4, 5)$. From Table 2 one can see that the classical limits on the initial momentum data are $(-\infty, -3)$. (The significance of $p = -3$ is that it is the critical value where $b_p = -p$; see (90).) The classical limits on initial position are $(9, \infty)$, in accord with (113). We choose $\gamma = 2$, so that the width of the packet in natural units is the same in both y and p space, and the effective supports of the initial wave packets (encompassing $\sim 95\%$ of the packet) for the position and momentum cases are $(\bar{y} - 2, \bar{y} + 2)$ and $(\bar{p} - 2, \bar{p} + 2)$, respectively. Thus (a) (112) is well satisfied for $\bar{y} \geq 4$; (b) the initial momentum-space packet is well inside the classically allowed region if $\bar{p} = -6$ (as we arbitrarily choose for the plots); (c) the initial position-space packet is well inside the classically allowed region if $\bar{y} \geq 11$. The computations indeed show that the two propagators give essentially equal results for $\bar{y} \geq 11$ but not for smaller $\bar{y}$. Our interpretation then is that the momentum-space calculation should be preferred for $4 < \bar{y} < 11$, and neither should be trusted for smaller $\bar{y}$. (The position-space solution might become superior when $\bar{p}$ is too close to an endpoint of a classically allowed interval of momentum, but we have not verified that.) In Figures 7 and 8 the two pieces of the position-space solution make spurious large excursions in the critical region $7 < \bar{y} < 11$ and then fall rapidly to 0 for smaller $\bar{y}$, as expected, since the y-space

Figure 7. Comparison of the evolution of initial wave functions by the WKB propagators associated with the classical direct paths. The initial data is such that $\gamma = 2$ and $\bar{p} = -6$. The final data is $(x, t) = (4, 5)$, so that $y_c = 9$. The average initial position, $\bar{y}$, is varied in the plot.

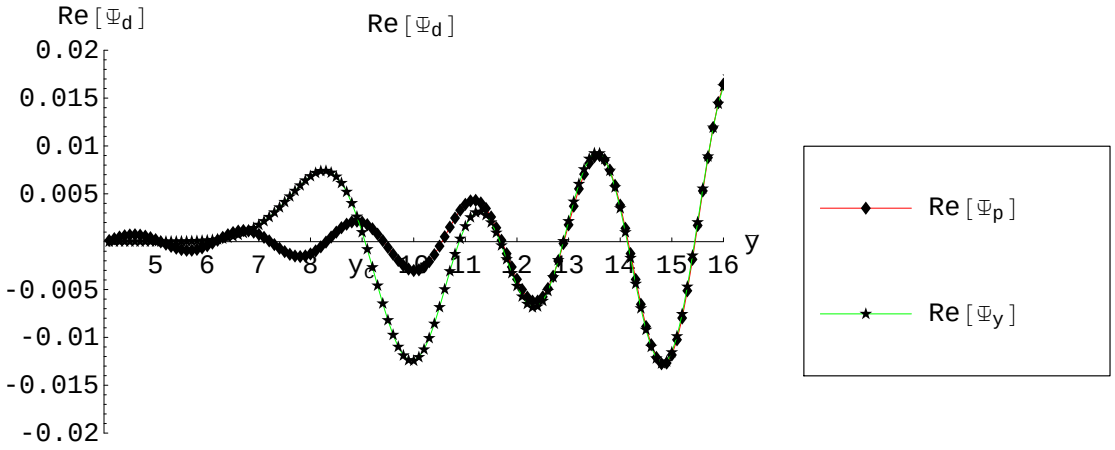

Figure 8. Comparison of the evolution of initial wave functions by the WKB propagators associated with the classical bounce paths. Again, $\gamma = 2$, $\bar{p} = -6$, $(x, t) = (4, 5)$, $y_c = 9$, and the average initial position, $\bar{y}$, is the independent variable.

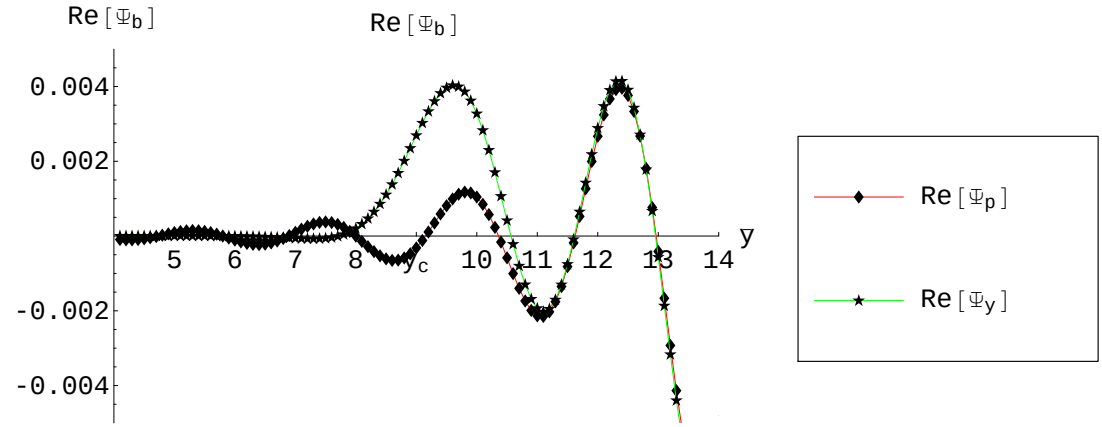

propagator is identically 0 in that region and the wave function is coming entirely from a wing of the Gaussian packet. The more trustworthy momentum-space solution is small but nontrivial in that region, again as expected.

Acknowledgments

We thank B.-G. Englert for help in solving the cubic equation (44) and S.-A. Chin for asking, "Why doesn't the method of images work?" This research has been supported in part by National Science Foundation Grants PHY-0554849 and PHY-0968269.

Appendix A. Why the method of images does not solve the problem

It is natural to expect that a Green function for a problem with a flat, perfectly reflecting boundary can be constructed from the Green function for all of space by subtracting the Green function for an image source located symmetrically on the other side of the boundary. When a potential function is involved, however, the situation is not as simple as it seems, especially when the derivative of the potential is not zero at the boundary.

In our problem (13), it is easy to fall into either of two traps.

First, we know the "free" propagator (19). It might seem that $U_{\rm free}(t,x,y) - U_{\rm free}(t,x,-y)$ is the propagator $U(t,x,y)$ for the scenario with the ceiling present, as it would be if the potential were absent. But this function does not satisfy the boundary condition, $U(t,0,y) = 0$. A source "uphill" does not have the same effect at the boundary as a source "downhill".

The second variant of the fallacy is to write $U_{\rm free}(t,x,y) - U_{\rm free}(t,-x,y)$. This time the boundary condition is satisfied, but the second term obeys the wrong differential equation (as a function of t and x), because the sign of the potential has been reversed.

The only correct way to apply the method of images is [20] to extend the potential to negative x as an even function: $V(x) = -|x|$. With the modified potential, $U_{\rm free}(t,x,y)$ will be invariant under simultaneous sign change of x and y, so that the two formulas proposed previously are equivalent and either satisfies the propagator problem. (The reflected term in the propagator presumably has as its semiclassical approximation the WKB contribution of the bounce paths.) Although indisputably correct, this construction is useless for our purposes, because solving the Schrödinger equation for the piecewise defined potential, $|x|$, is at least as hard as solving the original ceiling problem. Indeed, the standard textbook advice for solving a problem on the whole real line with an even potential is to decompose into odd and even modes, and to find the latter by solving the problem on the half-line with Dirichlet and Neumann boundary condition, respectively. Instead of solving the ceiling problem, the gambit has doubled it.

References

[1] Maslov V P and Fedoriuk M V 1981 Semi-Classical Approximation in Quantum Mechanics (Dordrecht: Reidel)

[2] Delos J B 1986 Semiclassical calculation of quantum mechanical wave functions *Adv. Chem. Phys.* **65** 161–214

[3] Littlejohn R G 1992 The Van Vleck formula, Maslov theory, and phase space geometry *J. Stat. Phys.* **68** 7–50

[4] Van Vleck J H 1928 The correspondence principle in the statistical interpretation of quantum mechanics *Proc. Natl. Acad. Sci. U.S.* **14** 178–188

[5] Keller J B and Rubinow S I 1960 Asymptotic solution of eigenvalue problems *Ann. Phys.* **9** 24–75

[6] Branson T P and Gilkey P B 1990 The asymptotics of the Laplacian on a manifold with boundary *Commun. Partial Diff. Eqs.* **15** 245–272

[7] Kirsten K 2001 Spectral Functions in Mathematics and Physics (Boca Raton:Chapman & Hall/CRC)

[8] Schaden M and Spruch L 2004 Diffraction in the semiclassical approximation to Feynman's path integral representation of the Green function *Ann. Phys.* **313** 37–71
[9] Gea-Banacloche J 1999 A quantum bouncing ball *Amer. J. Phys.* **67** 776–782
[10] Vallée O 2000 Comment on "A quantum bouncing ball" by Julio Gea-Banacloche *Amer. J. Phys.* **68** 672–673
[11] Goodmanson D M 2000 A recursion relation for matrix elements of the quantum bouncer *Amer. J. Phys.* **68** 866–868
[12] Keller J B 1962 Geometrical theory of diffraction *J. Opt. Soc. Amer.* **52** 116–130
[13] Zapata T 2007 The WKB Approximation for a Linear Potential and Ceiling *M. S. thesis* Texas A&M University, `http://hdl.handle.net/1969.1/ETD-TAMU-2112`
[14] Dean C E and Fulling S A 1982 Continuum eigenfunction expansions and resonances: A simple model *Amer. J. Phys.* **50** 540–544
[15] Carlitz R D and Nicole D A 1985 Classical paths and quantum mechanics *Ann. Phys.* **164** 411–462
[16] Holstein B R 1997 The linear potential propagator *Amer. J. Phys.* **65** 414–418
[17] Burdick M and Schmidt H-J 1994 On the validity of the WKB approximation *J. Phys. A* **27** 579–592
[18] Wolfram MathWorld 2004 Cubic formula `http://mathworld.wolfram.com/CubicFormula.html`.
[19] Namias V 1985 Simple derivation of the roots of a cubic equation *Amer. J. Phys.* **53** 775.
[20] Auerbach A and Schulman L S 1997 A path decomposition expansion proof for the method of images *J. Phys. A* **30** 5993–5995